13th World Conference on Earthquake Engineering
Vancouver, B.C., Canada
August 1-6, 2004
Paper No. 610

EXPERIMENTAL STUDY ON STRESS-STRAIN PROPERTY OF SHAPE MEMORY ALLOY AND ITS APPLICATION TO SELF-RESTORATION OF STRUCTURAL MEMBERS

Toshibumi FUKUTA[1], Masanori IIBA[2], Yoshikazu KITAGAWA[3], and Yuji SAKAI[4]

SUMMARY

Mechanical properties of shape memory alloy (hereinafter referred to as SMA) bars were investigated for their structural use of buildings and two examples of SMA in super elasticity phase applied to structural elements are proposed. The static and dynamic loading tests on SMA bars demonstrated that the stress-strain curve for tensile stress is completely different from that for compressive stress, irrespective of whether the load is static or dynamic in nature. Super elasticity was clearly evident under tensile strain of up to around 5%, but not under compressive strain, due to the presence of residual strain. The yield strength in compression is almost two times of tension yielding under the strain rate tested. SMA was applied to two structural elements in order to give a self-restoration and large deformability to building structures: SMA device for residential houses and concrete beam with SMA R-bars. Both applications were verified by seismic response analysis and model experiments to have a sufficient restoration capacity and large plastic deformability.

INTRODUCTION

SMA exhibits differing properties including a shape memory effect, super elasticity, and a behavior between the two according to the temperature of the material, as shown in Figure 1. Since SMA is known to have stable super elasticity within a temperature range of approximately 30 degrees centigrade above the reversible transformation temperature, this material has sufficient potential as a super elastic material for use in construction under the temperature of a construction environment, provided the transformation temperature is suitably controlled. It is already known that SMA wires exhibit super elasticity under tensile stress having a stress-strain curve shaped like a flag (Figure 2)[1-9]. Since SMA shows super elastic behavior over large strain ranges of up to about 5 %, a significant amount of deformation recovery is possible. This makes SMA a candidate material as a self-restoration member in structure if the transformation temperature can be suitably controlled. In consideration of the building structural use, the larger capacity of SMA will be needed than thin wires. Therefore, the mechanical properties of SMA bars

[1] Director of IISEE, Building Research Institute, Tsukuba, Japan, fukuta@kenken.go.jp
[2] National Institute of Land & Infrastructure Management, Tsukuba, Japan, iiba-m92hx@nilim.go.jp
[3] Professor, Keio University, Yokohama, Japan, kitagawa@sd-keio.ac.jp
[4] Master student, Keio University, Yokohama, Japan, vb07811@educ.cc.keio.ac.jp

are investigated in this study. Based on these results, two examples of SMA material in super elasticity phase applied to structural elements are proposed and its self-restoration capacity is verified by analysis and experiments.

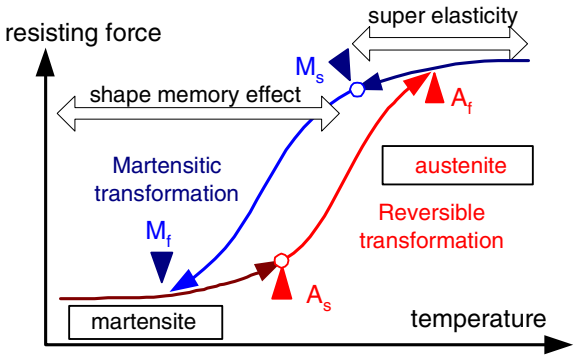

Figure 1 Transformation temperature and material phase

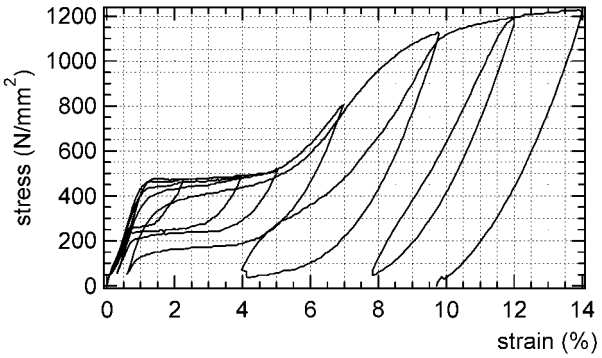

Figure 2 Stress-strain relation of SMA wire under room temperature 16 degree centigrade

STRESS-STRAIN PROPERTY OF SMA BARS

Loading test

Little is known about how SMA behaves when subjected to compression. This experiment was designed to determine the stress-strain relationship in SMA bars in super elastic alloy phase when subjected to compressive and tensile forces. The alloy composition and manufacturing conditions were carefully selected so that the experimental specimen would exhibit super elastic properties at room temperature. The exact composition was Ni 54.51%, Co 1.48%, and the remainder Ti. Table 1 shows transformation temperatures as measured using a differential scanning calorimeter.

The specimen was a 16 mm length of bar of diameter 7 mm, which was fabricated from a parallel section of a longer length of bar of diameter 17 mm. The top and bottom ends were clamped in hydraulic chucks with the centres perfectly aligned. Axial forces were then applied. (Hereunder, “specimen” refers to the parallel piece of 7-mm diameter bar.) To measure the strain on and temperature of the specimen, two strain gauges, one of which also doubled as a thermocouple, were affixed on either side of the center of the parallel section, and an 8 mm extensometer was attached across the gauges.

The ambient temperature was around 26 degree centigrade during the experiment. The readings from the two facing strain gauges were monitored to see whether the test piece was centrally loaded. The readings deviated from one another only very slightly during the experiment. Similarly, eccentricity under the compression load did not reach significant levels. Both static and dynamic loads were applied to the

specimen by controlling the distance between the chucks with respect to displacement and velocity. The load waveform used a triangular displacement-time relationship for both static and dynamic loads.

Table 1 Transformation temperature of SMA bar tested

transformation temperature	Martensitic transformation start temperature	Martensitic transformation end temperature	Reversible transformation start temperature	Reversible transformation end temperature
centigrade	Ms=25.5	Mf=-19.0	As=8.9	Af=43.2

Static tensile property

Figure 3 shows the stress-strain relationship for the static tensile test. The experiment began with three repetitions at each level (0%–1%, 0% –2%, etc.), as shown by the solid line. The specimen was then placed in a hot water bath at 50 degree centigrade (hotter than the temperature at the end of the reverse transformation) for ten minutes, and repetitions were performed during unloading (at 0% – 2%, 2% – 4%, etc.). The strain generally returned to zero after each loading, clearly indicating super elastic properties. Strain hardening can be observed from around 4% strain, where the curve gradient starts increasing. A very small amount of residual strain was observed after removal of the strain (approximately 4.5%).

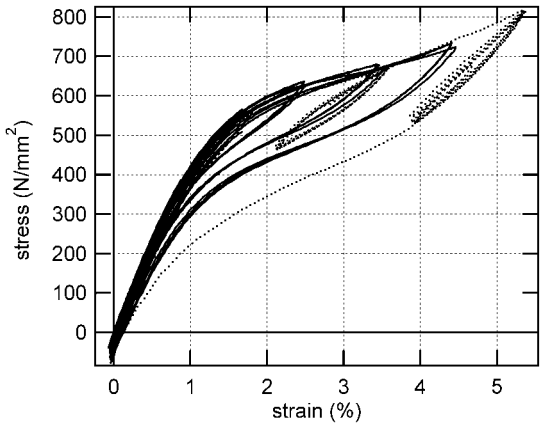

Figure 3 Stress-strain relations for static tension test

Static compressive property

As Figure 4 shows, the experiment was conducted in two stages. The first stage consisted of three repetitions at each of the target strain values: 0% – 1%, 0% – 2%, 0% – 3%, 0% – 4%, and 0% – 5% (actually closer to 6%). The specimen was then placed in hot water (50 degree centigrade) for ten minutes, and three repetitions were performed at each of the following target strain values: 0% – 2%, 2% – 4%, and 4% – 6%. Since the load was controlled by the distance between the two chucks, the paths or trajectories the stress-strain curve took were not exactly the same for all the sets of tests, because of the residual strain that remained in the test piece after removal of the load.

Figure 4 shows the results of both the first half of the experiment (solid line) and the second half (broken line), with the second half results shifted in parallel with the strain axis at the conclusion of the first half. The stress-strain curve for compression forces differs in shape from the tension curve in Figure 3. The strain value shows no sign of the super elasticity which would cause it to revert to zero upon removal of the load. The residual strain in fact resembles the stress-strain relationship for cold-formed carbon steel.

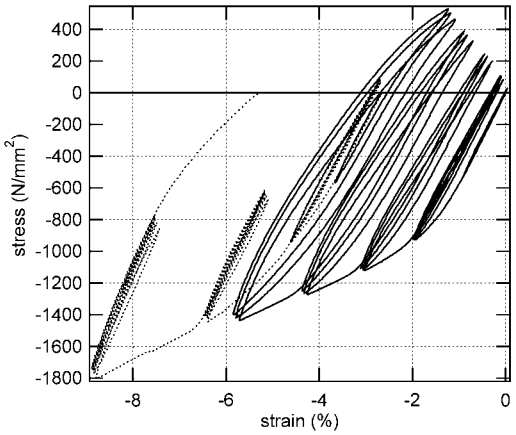

Figure 4 Stress-strain relation for static compression test

Static tensile-compressive property

Figure 5 shows the results of the tensile-compressive tests. The stress-strain relationship differs in many respects (yield strength, rigidity of plateau area after yielding, final strain value after removal of load) between the tension and the compression tests. Residual strain was observed after compression, but this could be negated almost completely by then applying a tensile strain that was greater (in absolute terms) than the compression strain that caused the residue.

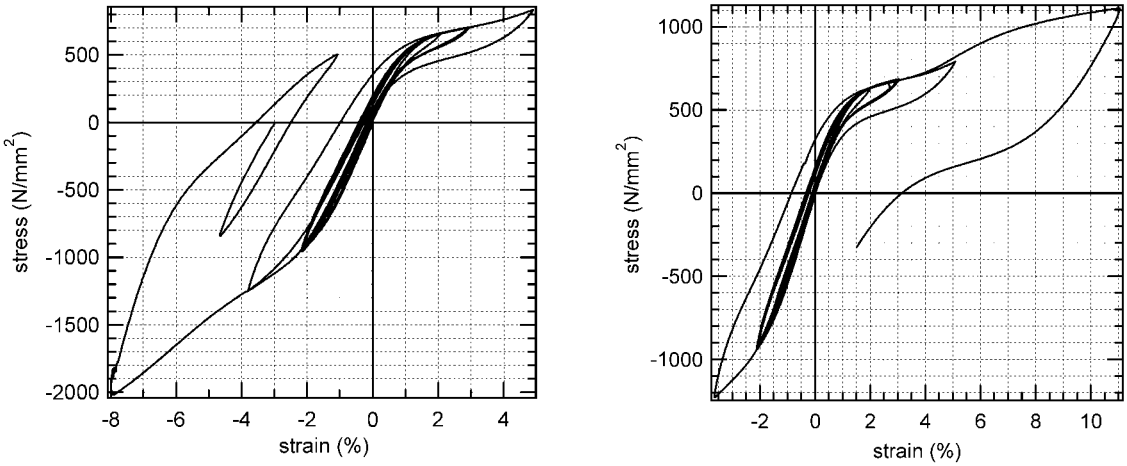

a) for static compression-tension **b) for static tension-compression**

Figure 5 Stress-strain relation for static compression-tension

Dynamic tensile-compressive property

Energy absorption under cyclic loading

The load waveform was triangular. The amplitude was varied at ±1%, ±2%, and ±4%, in that order. Four different loading frequencies (0.066 Hz, 0.33 Hz, 1.64 Hz, and 3.3 Hz) were used at each amplitude. Ten repetitions were performed for each set of conditions. Figures 7-a and 7-b represent the repetition loop area E shown in Figure 6 divided by the area Eo of the rectangle inscribed by the loop, for 2% and 4% amplitude, respectively. Energy absorption per cycle was determined by comparing the loop area for a single cycle with the area of the rectangle that circumscribes the loop, as described above. (The equivalent attenuation method cannot be applied directly in this situation due to differences in the load-carrying capacity at peak times between the tension and compression sides in the stress-strain curve for SMA.) The

energy absorption rate per cycle differs according to the strain amplitude: at 2% strain amplitude, the higher strain velocity causes the energy absorption rate to decrease, while at 4% strain amplitude, there was no simple correlation between the strain velocity and the rate of energy absorption.

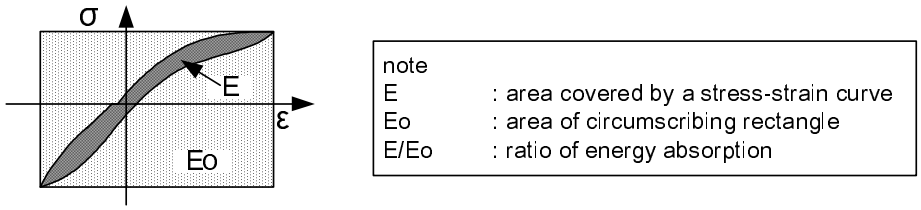

Figure 6 Definition for E/Eo

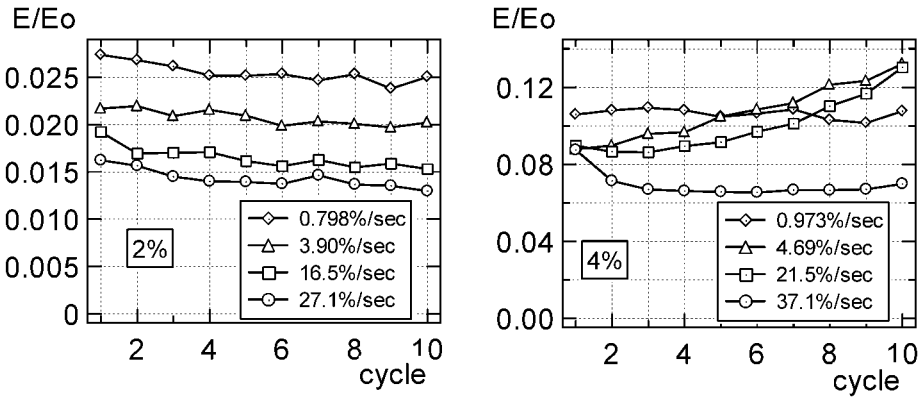

a) for 2% amplitude of strain **b) for 4% amplitude of strain**

Figure 7 E/Eo vs. loading cycle

Strain rate effects on Young's modulus & yield strength

Figure 8 presents effects of strain rate on Young's modulus and yield strength defined as 0.2 % offset value. The obvious relation cannot be notified between strain rate and these values. Yield strength in compression is almost two times of tension yielding under the strain rate tested.

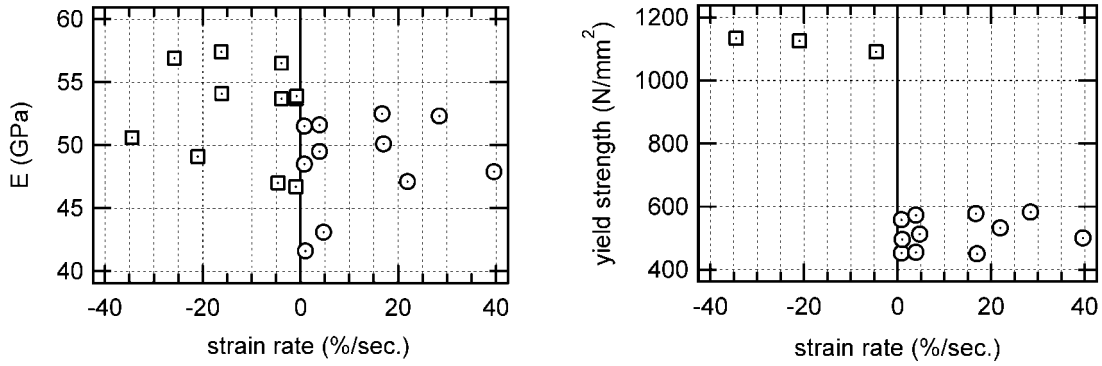

a) Young's modulus vs. strain rate **b) Yield strength vs. strain rate**

Figure 8 Effect of strain rate on Young's modulus & yield strength

SMA DEVICE FOR RESIDENTIAL HOUSES

Brace type SMA device

SMA bars clearly show super elasticity in tension and not in compression. If SMA bars are used as a tension member, it would effectively control a displacement response of structures and return their lateral drift to zero after earthquakes. Then, a response control device with SMA bars is designed for low-storied houses as the followings: 1) SMA devices carry lateral forces, and beam-to-column frame supports vertical loads, 2) the size of SMA bars is designed so that the device has its required lateral stiffness and strength, 3) SMA bars are effective only in tension, 4) elastic design is applied to the other part (i.e. steel frame and joints) of the device under the yield strength of SMA bars (see Figure 9).

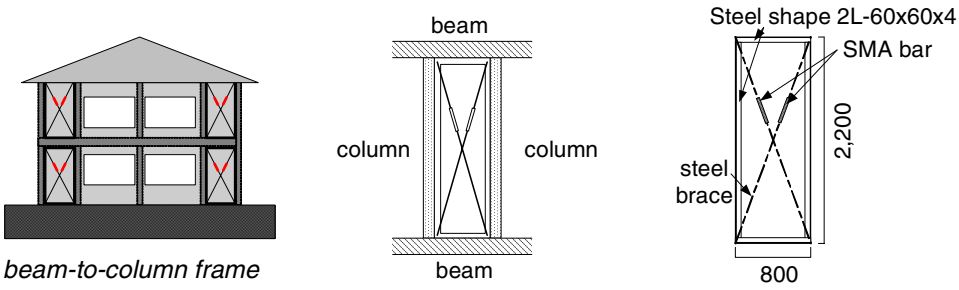

Figure 9 SMA device and its set up into a beam-to-column frame

Seismic response of structure with SMA device

In order to conform the performance of SMA devices under sever earthquakes, the response of a structure with SMA devices was analyzed to El Centro NS wave of 340 gals maximum input. It is assumed that beam-to-column joints of the frame are pin-joint, the frame of the device behaves in elastic and the braces work only in tension. Therefore the restoring force characteristic of the structure can be assumed to be similar to stress-strain curve of SMA, as shown in Figure 10-b. This multi-linear model is based on the material test result of SMA bar introduced in the former chapter (see Figure 10-a). A single degree of freedom model with 0.5 second natural period, 5% viscous damping and lateral yield shear Qy of 40% of total structure weight was selected as an analytical model, which represents low-storied houses. The response is drawn in Figure 11 in comparison with the system of bi-linear restoring force characteristics. The analysis demonstrates that SMA devices return lateral drift of the structure to zero, on the contrary bi-linear system has some amount of story drift after the quake. But the maximum lateral displacement of the structure with SMA devices is about 1.5 times of the bi-linear model, because of lack of energy dissipation.

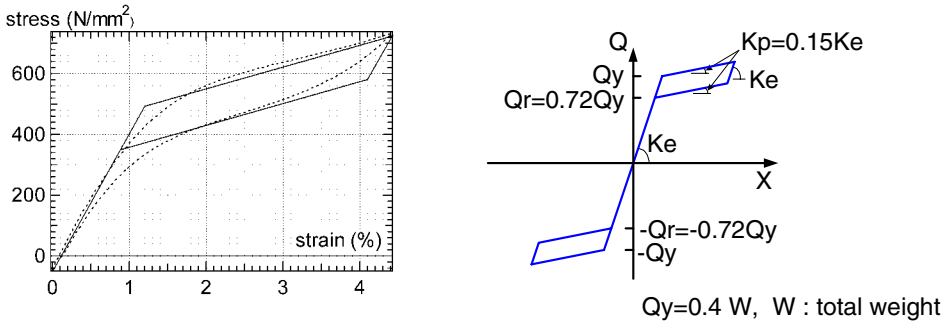

a) Stress-strain curve of SMA bar **b) Restoring characteristic model**

Figure 10 Restoring characteristic model of a structure with SMA devices

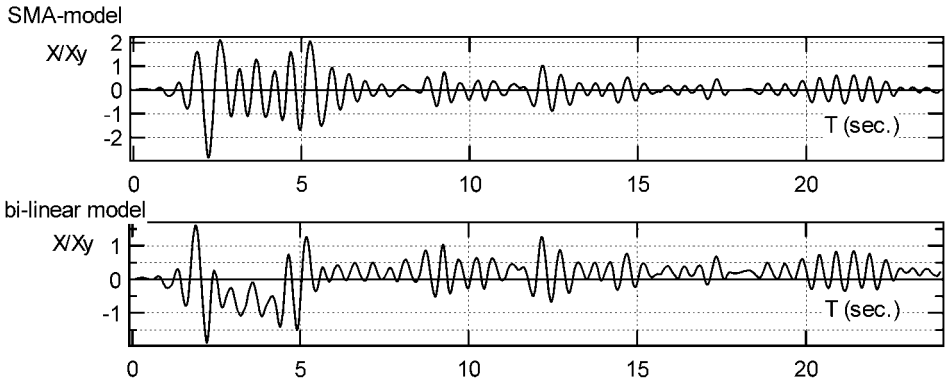

Figure 11 Time history of response of SMA-model & bi-linear model

SELF-RESTORATION CONCRETE BEAM WITH SMA R-BARS

Self-restoration by SMA R-bars

Figure 12 presents the RC coupled wall system connected by joint beams, which should be deformed largely under the lateral drift of the system. Providing SMA R-bars are arranged in the joint beams, SMA can take advantage of the super elasticity as a capability that will allow structures to recover from large deformation. In order to verify the capability, model mortar beam tests were conducted.

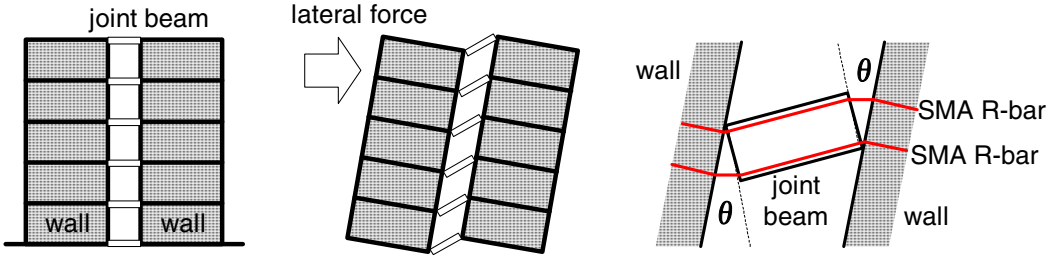

a) Coupled wall system b) Drift under lateral force c) Deflection of joint beam

Figure 12 Deformation of coupled wall system under lateral force

Loading test of mortar-beam with SMA R-bars

SMA wires having a length of 500 mm and a diameter of 2.0 mm were selected as the materials with the maximum diameter obtainable. The transformation temperature was set to exhibit super elasticity at room temperature. Since SMA wires having a diameter of 2.0 mm were used as the main bars, mortar was used instead of concrete. The test specimens were formed to have a square cross-section with 100-mm sides. For comparison purposes, a test specimen was prepared using steel wire (cold-formed) with a diameter of 1.9 mm as the main bars. Figure 13 shows the details and dimensions of the specimens. Since the super elasticity of the SMA makes the bending process difficult, steel blocks were provided on the ends of the beam and the main bars were fixed in holes in the steel blocks through the frictional forces generated among screws, the steel blocks, and the wires. The tests confirmed that the SMA wires did not come out of the steel blocks prior to tensile fracture of the wires. Figures 2 and 14 show the stress-strain relationship of the SMA wires and steel wires, while Table 2 lists the mechanical properties of the material. Here, Young's modulus of the SMA wires is about 1/4 that of the steel wires and the yield strength is about 17% less. A simple bending test was conducted in which a concentrated load is applied to the mid span of the beam orthogonal to the material's axis, while both ends of the specimen are supported by pins.

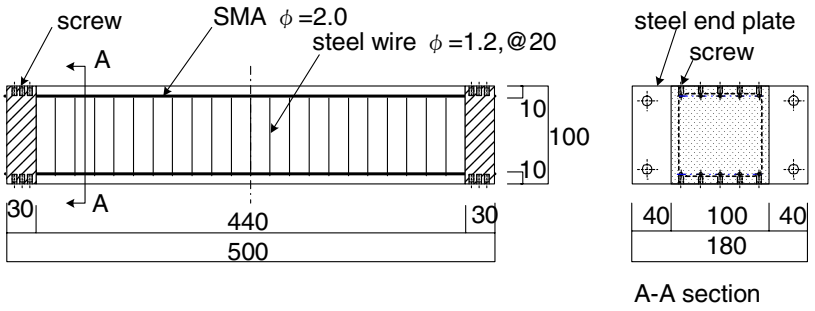

Figure 13 Detail of test specimen SMA-5

Table 2 Mechanical properties of material (unit : N/mm^2)

Material	Young's modulus	Yield strength	Maximum strength
SMA wire	39,000	480	1,220
Steel wire	177,000	576	576
Mortar	20,000	-	26.5

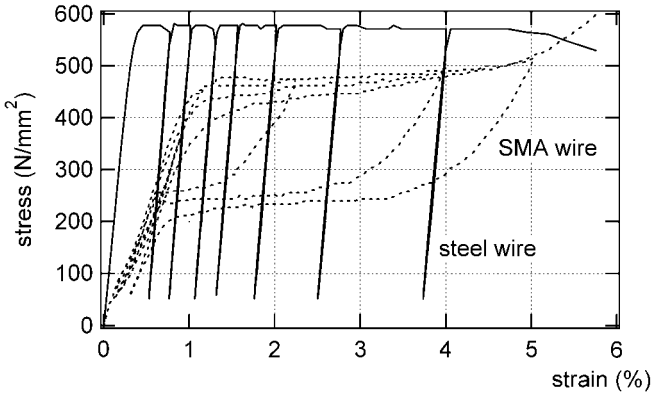

Figure 14 Stress-strain relation of steel wires in comparison with a part of SMA wire's curve

Load carrying property of mortar-beam with SMA R-bars

Figure 15 shows the load-deflection (rotation angle of the material ends) relationship for each test specimen. In the test specimen using SMA bars (SMA5), an abrupt load loss occurred directly after a crack was generated, since the mortar had no more resistance to tensile stress. As deflection increased after this point, the SMA bars began to take on the burden of the tensile stress and gradually increased in resisting force. Residual deflection after unloading was small, even when the deflection was large at the loading peak. The specimen reached a maximum strength when the rotation angle of its ends was 0.13 radians. At the maximum strength, compressive failure occurred in the mortar around the loading point in the center of the beam. However, the SMA bars did not rupture. The deforming capacity of the SMA wires at their maximum strength exceeded ten times that of the beam using steel wires (STE).

The test specimen with steel wires as main bars had rigidity during unloading approximately equivalent to elastic stiffness, while showing a tendency to increase in deflection during hysteresis peaks and to increase in residual deflection after unloading. The test specimen reached its ultimate strength at a rotation angle of 0.008 radians. Subsequently, the resisting force began to degrade and, at a rotation angle of 0.016 radians, main bars in the center of the beam ruptured in the tension side.

Since an external transverse force was applied to the center of the simply supported beam, a single crack was generated on the tension side around the critical section of the beam for two specimens. The crack width increased along with an increase in deflection caused by the applied force. Figure 16 shows the

variations in crack widths for each test specimen. The residual crack widths after unloading were roughly uniform in SMA5, with no relation to the crack widths during hysteresis peaks. On the other hand, residual crack widths tended to increase in the specimen using steel wires as main bars along with an increase in the generated crack widths.

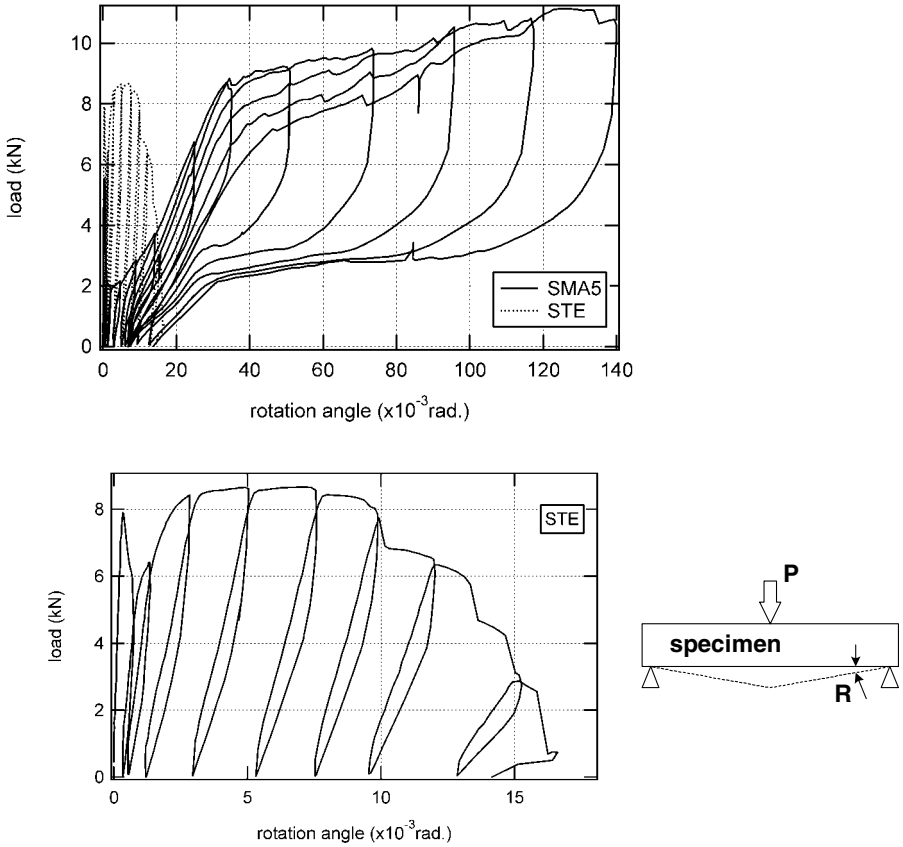

Figure 15 Load vs. rotation angle of the beams

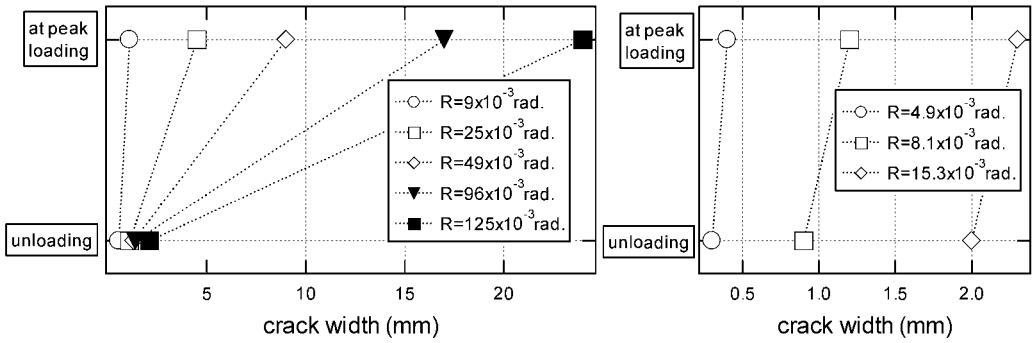

a) beam (SMA5) with SMA wires **b) beam (STE) with steel wires**

Figure 16 Crack width at the center of the beam

CONCLUSION

This study first looked at the stress-strain relationship of Ti-Ni shape memory alloy for a columned specimen. The experiment was conducted with the specimen at the super-elastic-alloy-phase temperature. The specimen was subjected to static and dynamic compressive and tensile stress. The test results demonstrated that the stress-strain curve for tensile stress is completely different from that for compressive stress, irrespective of whether the load is static or dynamic in nature. Super elasticity was clearly evident under tensile strain of up to around 5%, but not under compressive strain, due to the presence of residual strain. The yield strength in compression is almost two times of tension yielding under the strain rate tested.

Second, SMA was applied to two structural elements in order to give a self-restoration and large deformability to building structures. The braced frame type devices with SMA were designed to control seismic response of residential houses. Their performance was verified by seismic response analysis to return story drift of structures to zero after earthquakes, effectively.

The mortar beam with SMA wires was examined to verify the potential self-restoration capacity. The test results revealed that the beam with SMA wires almost recovered after incurring an extremely large deformation, in comparison with that of the beam with steel wires. This result suggests that the SMA R-bars is added self-restoration capacity to concrete beams.

ACKNOWLEDGMENTS

This study was carried out by the Effector Technology Section (led by University of Tokyo professor Takashi Fujita) of the Super-Intelligent Construction Systems Development Project, a joint research project between Japan and the United States. The SMA material used in experiments was provided by Daido Steel Co., Ltd.. The authors wish to convey their thanks to all involved

REFERENCES

1. Fukuta T., Iiba M., Kitagawa Y., Syugo Y. “Experimental Results on Stress-Strain Relation of Ni-Ti Shape Memory Alloy Bars and Their Application to Seismic Control of Buildings”, 3rd WSCS, Italy, April, 2002.

2. Tamai H., Kitagawa Y. “Pseudoelastic Behavior of Shape Memory Alloy Wire and Its Application to Seismic Resistance Member for Building”, IWCMM 10, Galway, Ireland, Aug, 2000.

3. Graesser E.J., Cozzarelli F.A. “Shape-Memory Alloys as New Material for Aseismic Isolation”, ASCE Journal of Engineering Mechanics, Vol. 117, No. 11, 1991.

4. Witting P.R., Cozzarelli F.A. “Shape Memory Structural Dampers: Material Properties, Design and Seismic Testing”, Technical Report NCEER-92-0013, State University of New York, Buffalo (USA), 1992.

5. Hodgson, Krumme R.C. “Damping in Structural Applications”, Proceeding of the 1st International Conference on Shape Memory and Superelastic Technologies, Pacific Grove, California (USA), 1994.

6. Whittaker A.S., Krumme R.C., Hayes J.R. “Structural Control of Building Response using Shape Memory Alloys”, Headquarters U.S. Army Corps of Engineers, Washington D.C. 1995.

7. Dolce M., Marnetto R. “MANSIDE: Seismic Devices Based of Shape Memory Alloys”, MANSIDE Project –Final Workshop- Memory Alloys for Seismic Isolation and Energy Dissipation Devices, Rome, January 28-29, 1999.

8. Cardone D., Dolce M., Nigro D. “MANSIDE Project –Final Workshop- Memory Alloys for Seismic Isolation and Energy Dissipation Devices”, Rome, January 28-29, 1999.

9. Funakubo H. and et.al. ”Shape Memory Alloy”, Sangyo Tosho Co., 1984.6 (in Japanese).